Biochimica et Biophysica Acta, 1063 (1991) 162–170

ADONIS 000527369100148F

BBAMEM 75170

Physicochemical determinants for the interactions of magainins 1 and 2 with acidic lipid bilayers

Katsumi Matsuzaki, Mitsunori Harada, Susumu Funakoshi, Nobutaka Fujii and Koichiro Miyajima

Faculty of Pharmaceutical Sciences, Kyoto University, Sakyo-ku, Kyoto (Japan)

(Received 21 June 1990)
(Revised manuscript received 20 November 1990)

Key words: Magainin; Acidic lipid membrane; Binding isotherm; Electrostatic interaction; Membrane fluidity; Secondary structure

Permeability enhancement of acidic lipid small unilamellar vesicles (dioleoylphosphatidylglycerol, DOPG; dipalmitoylphosphatidylglycerol, DPPG; bovine brain phosphatidylserine, PS) induced by magainins 1 and 2, basic antimicrobial peptides from *Xenopus* skin, was investigated at 30°C based on leakage of calcein, an entrapped fluorescent marker. Both the peptide concentration and the lipid concentration dependencies of the leakage rate were analyzed to obtain the binding isotherms of the peptides to the membranes and the 'membrane-perturbing activities' of the membrane-bound peptides. For both peptides, the binding affinity was in the order DOPG > DPPG > PS, which coincided with the zeta potential order (−54, −39, and −9 mV, respectively). An increase in salt concentration of the medium reduced binding and leakage. Electrostatic interactions play a crucial role in the binding process. On the other hand, the membrane-perturbing activity is regulated by membrane fluidity: The fluid membranes (DOPG and PS) were leakier. A circular dichroism study suggested that at least 14 positively charged residues in the N-terminal regions can form amphiphilic helices which interact with the membranes. An even stronger binding of magainin 2 can be explained in terms of more positive charges in its N-terminal region. A tentative model for the magainin–lipid interactions is hypothesized.

Introduction

Magainins 1 and 2, recently isolated from *Xenopus* skin, are basic antimicrobial peptides with broad spectra: NH_2-Gly-Ile-Gly-Lys-Phe^5-Leu-His-Ser-Ala-Gly^{10} (for magainin 1, Lys^{10} for 2)-Lys-Phe-Gly-Lys-Ala^{15}-Phe-Val-Gly-Glu-Ile^{20}-Met-Lys (for 1, Asn for 2)-Ser-COOH The peptides are considered a part of the defense system in the vertebrate [1,2]. Westerhoff et al. have shown that the dissipation of the electric potential of bacterial membranes and the resultant uncoupling of respiration are possible action mechanisms [3–5]. The idea that membranes are primarily a site of action is supported by additional findings: magainin 2 ruptures protozoas [1,2] and forms a voltage-gated ion channel in a planar lipid membrane [6,7]. The membrane affinity seems to arise from amphiphilic helical conformations of the peptides, as proposed by their primary structures. A structure-activity relationship study [8] revealed that analog peptides with increased helical contents exhibit significantly enhanced antimicrobial activities, although the helical contents were estimated in a trifluoroethanol/water mixture, an improper medium for representing the polar–nonpolar interfacial property of membranes.

Liposomes, a simple model for biomembranes, are a useful system for molecular level elucidation of peptide-lipid interactions: The change in membrane permeability can be correlated to conformational changes in both peptides and lipids, as detected by various spectroscopic and thermal techniques [9–13]. We have demonstrated [12] that magainin 1 interacts specifically with acidic lipid vesicles, through electrostatic interactions followed by hydrophobic interactions, to form an amphiphilic helix, inducing leakage of a fluorescent dye, calcein, entrapped within the liposomes. Furthermore, we have estimated [12] two sets of

Abbreviations: DPPG, L-α-dipalmitoylphosphatidyl-DL-glycerol sodium salt; DOPG, L-α-dioleoylphosphatidyl-DL-glycerol sodium salt; PS, L-α-bovine brain phosphatidyl-L-serine; SUVs, small unilamellar vesicles; CD, circular dichroism; NRMSD, normalized root mean standard deviation; DSC, differential scanning calorimetry.

Correspondence: K. Miyajima, Faculty of Pharmaceutical Sciences, Kyoto University, Sakyo-ku, Kyoto, 606, Japan.

data to characterize the peptide induced leakage for bovine brain phosphatidylserine sonicated vesicles: the binding isotherm of the peptide to the membranes and the 'membrane-perturbing activity' of the peptide (the amount of membrane-bound peptide per lipid molecule necessary for leakage). Such a detailed analysis serves a quantitative comparison between peptide–lipid interactions in various systems.

In this study, we examined the susceptibility of phosphatidylglycerols, abundant acidic lipids in bacterial membranes [14], to magainin 1 to elucidate the effects of the surface potential and fluidity of the membranes on the peptide–lipid interactions. In addition, we extended this quantitative analysis to magainin 2 to clarify the cause of its stronger antibiotic activity [2]. We found that electrostatic interactions determine the affinity of the peptides to the membranes whereas the membrane fluidity influences the membrane perturbing activity. Based on these leakage results and data from circular dichroism (CD) and differential scanning calorimetry (DSC) we will hypothesize a tentative model for the magainin–membrane interactions.

Materials and methods

Materials. Magainin 2 was synthesized by a *t*-butoxycarbonyl based solid phase synthesis as was magainin 1 [12]. The purity of synthetic magainin 2 was ascertained by amino acid analysis, after a leucine aminopeptidase (Sigma, L-6007) digestion [12]. Amino acid ratios in the digest were: Ser, 1.99 (2); Glu, 1.00 (1); Gly, 3.64 (4); Ala, 1.98 (2); Val, 0.95 (1); Met, 0.93 (1); Ile, 1.72 (2); Leu, 0.93 (1); Phe, 2.92 (3); Lys, 3.91 (4); His, 0.89 (1); Asn, n.d. (recovery of Glu was 91%). The concentrations of the peptides were based on quantitative amino acid analysis (In our previous study [12], we overestimated the peptide concentration by a factor of approx. 1.4.). L-α-Dipalmitoylphosphatidyl-DL-glycerol, sodium salt (DPPG), L-α-dioleoylphosphatidyl-DL-glycerol, sodium salt (DOPG), and L-α-bovine brain phosphatidyl-L-serine (PS) were purchased from Sigma. Calcein (3,3′-bis-[*N*,*N*-bis(carboxymethyl) aminomethyl]-fluorescein) and spectrograde organic solvents were supplied by Dojin (Kumamoto, Japan). Ammonium *d*-camphor 10-sulfonate was a product of Katayama (Osaka, Japan). All other chemicals were obtained from Wako (Tokyo, Japan). A 10 mM Tris-HCl/150 mM NaCl/1 mM EDTA buffer (pH 7.0) was prepared with water twice-distilled in a quartz still.

Leakage from small unilamellar vesicles (SUVs). Calcein-entrapped SUVs were prepared by a sonication-gel filtration method as described elsewhere [12,13]. Briefly, lipid films, after an overnight vacuum drying, were hydrated with a 70 mM calcein solution (pH 7.0). The suspensions were vortexed, followed by sonication in ice-water (at 60°C for DPPG) with nitrogen bubbling for 20 min by using a titanium tip sonicator (Tomy UD-200). After centrifugal metal-debris removal, untrapped calcein was removed by gel filtration (Sephadex G-50, the buffer being used as an eluent). The separated vesicles were mixed with calcein-free sonicated vesicles to obtain the desired lipid concentration. The lipid concentration was determined by phosphorus analysis [15]. The vesicular suspension (0.3 ml) was added to 2.7 ml of a magainin 1 or 2/buffer solution under stirring in a thermostated (30 ± 0.5°C) quartz cuvette. In some experiments the NaCl concentration in the buffer was modified. The leakage of calcein from the vesicles was monitored fluorometrically (excitation at 490 nm and emission at 520 nm, [16]) on a Jasco FP-550 spectrofluorometer. The fluorescence intensity corresponding to 100% leakage was determined by adding 0.1 ml of a 10% v/v Triton X-100 aqueous solution to 3 ml of the sample. Percent leakage was calculated after correcting volume due to dilution.

Zeta Potential. SUVs in the buffer were prepared by a sonication of hydrated lipid films under nitrogen bubbling in ice-water (for DPPG, at 60°C) followed by centrifugal metal-debris removal [12,13]. The zeta potentials of the SUVs were calculated by using Smoluchowski's equation [17] from their electrophoretic mobilities measured on a Photal ELS-800 electrophoretic light scattering spectrophotometer [18]. The scattering angle was 15° or 12.5° and the electric field intensity was −15.19 to −15.60 V/cm. The true electrophoretic mobilities at a stationary level were evaluated by measuring apparent mobilities at seven different positions along the depth axis of the cell wall [18].

CD. The CD spectra of a 17 μM peptide/buffer solution in the absence and presence of SUVs (lipid concentration: 306 μM for DPPG, 641 μM for DOPG, and 400 μM for PS) were recorded on a computerized Jasco J-600 instrument in a wavelength range 240–195 nm. The instrumental outputs were calibrated with non-hygroscopic ammonium *d*-camphor 10-sulfonate [19]. A quartz cuvette of 1-mm path length was thermostated at 30 ± 0.5°C. Eight scans were averaged for each sample. Averaged blank spectra (the vesicle suspensions or the buffer) were subtracted to yield the 'pure' spectra of the peptides. The reported spectra were the average of three independent preparations for each type of sample. The coefficients for variation were less than 5% above 200 nm yet as large as 20% near 195 nm due to the presence of salt. Thus, the data in the range 240–200 nm were employed to calculate the secondary structures of the peptides by using a constrained least-squares algorithm [20] with a set of reference spectra by Chang et al. [21]. The helical length was chosen as described previously [22].

Titration study. A magainin 1 (1.4 or 0.7 μM)/buffer solution (10 mM Tris-HCl/1 mM EDTA/150 or 500

mM NaCl, pH 7.0) was titrated with small aliquots of a 4 mM DOPG SUV suspension in a 10-mm path length quartz cuvette thermostated at 30 ± 0.5°C. Ellipticity at 222 nm was recorded on the CD apparatus. The reported values are the averages of 640 data points measured at 0.1 s time intervals. The standard deviation of the signal fluctuation was approx. 300 deg cm^2 $dmol^{-1}$. Blank values (the vesicles were added to the buffer) were subtracted to obtain the peptide signal. Base line drift was monitored by checking the ellipticity value at 260 nm.

DSC. Aliquots of a DPPG/chloroform/methanol solution were placed in a test tube. After evaporation of the solvent, the residual film was dried under vacuum overnight. Peptide/buffer solutions or the buffer was added onto the film, and the suspension was vortexed at 60°C. The vesicles thus prepared were cooled to room temperature and then reheated to 60°C. The cooling-heating process was repeated twice. A DSC thermogram of the suspension (30 μl) in a sealed aluminum pan was measured at a heating rate of 2 C°/min against the buffer as a reference on a computerized Shimadzu DSC-50 instrument. The heat and temperature outputs were calibrated with 99.99% gallium (m.p., 302.9 K; enthalpy of melting, 5.589 kJ/mol). The lipid and peptide concentrations were 40 and 1.4 mM, respectively.

Results

Leakage

Fig. 1 shows the time courses of magainin 1 (10 μM) induced calcein leakage from the acidic lipid SUVs at 30°C (The lipid concentrations were 186–203 μM). The lipids exhibited differences in susceptibility to the antimicrobial peptide in the order DOPG > PS > DPPG. The lowest sensitivity value of DPPG may be ascribed to the rigidity of the membrane. However, a significant difference between the fluid bilayers, i.e., the DOPG and the PS membranes, suggests the contribution of another factor. Elucidation of the determinants of the difference in susceptibility is the main purpose of this study.

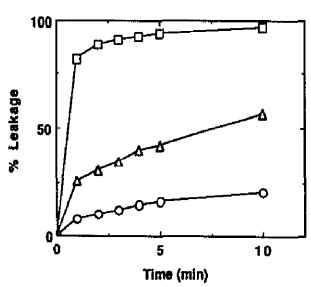

Fig. 1. Time-course of magainin 1 induced calcein leakage from acidic lipid SUVs at 30°C. The leakage of the dye was monitored fluorometrically. Acidic lipids: circles, DPPG; squares, DOPG; triangles, PS. The peptide and the lipid concentrations were 10 and 186–203 μM, respectively.

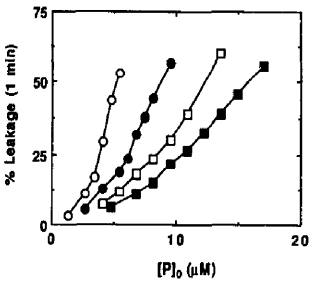

Fig. 2. Dependence of calcein leakage rate on peptide and lipid concentrations for magainin 2-PS system at 30°C. The calcein leakage rate, defined as the percent leakage for the initial 1 min, is plotted as a function of the peptide concentration $[P]_0$, at different lipid concentrations [L]. [L] (μM): open circles, 46; closed circles, 91; open squares, 135; closed squares, 181.

Membrane-lytic peptides alter lipid membrane permeability in two steps, i.e., the binding of the peptide to the membrane and the ensuing membrane disruption. Accordingly, two determinants of the leakage are (1) the membrane affinity of the peptide (the binding isotherm) and (2) its membrane-perturbing activity. These factors can be obtained by analyzing both the peptide concentration and the lipid concentration dependencies of the leakage rate [12,13]. Fig. 2 shows the data for the magainin 2-PS system as an example. An increase in the peptide concentration or a decrease in the lipid concentration resulted in an enhanced leakage rate, suggesting that the amount of membrane-bound peptide per lipid molecule, r, determines the leakage rate. Here the leakage rate defined as the percent leakage for the initial 1 min is used as a measure of the initial leakage rate because the true rate was too rapid to measure precisely without a stopped-flow apparatus. The amount, r, can be connected to experimental conditions (the peptide concentration, $[P]_0$, and the lipid concentration, [L]) through a material balance equation:

$$[P]_0 = [P]_f + r[L] \quad (1)$$

where $[P]_f$ is the free peptide concentration. A pair of r and $[P]_f$ values corresponding to a given leakage rate can thus be estimated with four sets of $[P]_0$ and [L] where the leakage rate was observed. Fig. 3 shows that the $[P]_0$ vs [L] plots at any given leakage rates gave linear relations (the square correlation coefficients were grater than 0.95). The r and $[P]_f$ values were obtained from the slopes and the intercepts, respectively. Fig. 4a shows the r-$[P]_f$ relationship thus estimated (i.e., the binding isotherm) with data for the other systems. The uncertainties, due to the indirect determination, in the

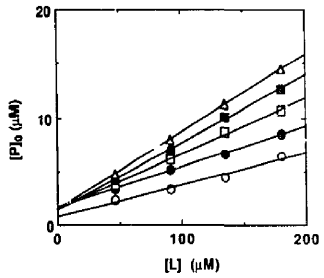

Fig. 3. Estimation of free and membrane-bound peptide concentrations. Four pairs of $[P]_0$ and [L] values where a given leakage rate was observed were obtained from Fig. 2. $[P]_0$ is plotted against [L] according to Eqn. (1). The free peptide concentration, $[P]_f$, and the amount of membrane-bound peptide per lipid molecule, r, were evaluated from the intercept and the slope, respectively. Leakage rate (the percent leakage for the initial 1 min): open circles, 10; closed circles, 20; open squares, 30; closed squares, 40; triangles, 50. The lines are the least-squares fits.

$[P]_f$ and the r values were estimated to be $\pm 20\%$ and $\pm 10\%$, respectively. In Fig. 4b the leakage rate is plotted as a function of r. In the case of the solid DPPG vesicles from which the leakage was rather slow, the rate was expressed as the percent leakage for 5 min. To check the reproducibility, we repeated the experiment for the magainin 2-PS system and found the r-$[P]_f$ and the percent leakage-r relationships to be superimposable onto those in Figs. 4a and 4b.

Binding isotherms can be obtained on the basis of changes in some physicochemical properties of peptides, e.g., ellipticity, upon membrane binding. We estimated the isotherm for the magainin 1-DOPG system by adding the vesicles to a fixed concentration (1.4 μM) of the peptide and measuring the ellipticity at 222 nm. The data (Fig. 5a) were analyzed with the method of Beschiaschvili and Seeling [23]. A two-state model, assumed in the analysis, seems to be valid because experimenting at a different concentration (0.7 μM) of the peptide gave identical results (data not shown). Fig. 5b combines data from the binding isotherms in buffers containing 150 mM NaCl (open circles) and 500 mM NaCl (squares) with the data obtained from the leakage experiment (closed circles), replotted from Fig. 4a. The isotherms estimated from the two different methods (leakage and CD) were very similar, guaranteeing the validity of the leakage method.

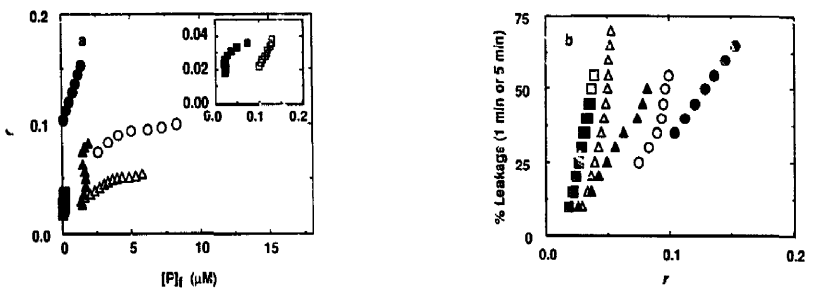

Fig. 4. Quantitative analysis of magainins 1 and 2 induced leakage at 30°C. The relationships (a) between the amount of membrane-bound peptide per lipid molecule, r, and the free peptide concentration, $[P]_f$, (i.e., binding isotherms) and (b) between the leakage rate and r are shown. The leakage rate for solid DPPG vesicles is expressed as the percent leakage for 5 min. Peptides: open symbols, magainin 1; closed symbols, magainin 2. Lipids: circles, DPPG; squares, DOPG; triangles, PS. The inset in (a) is a magnification near the origin.

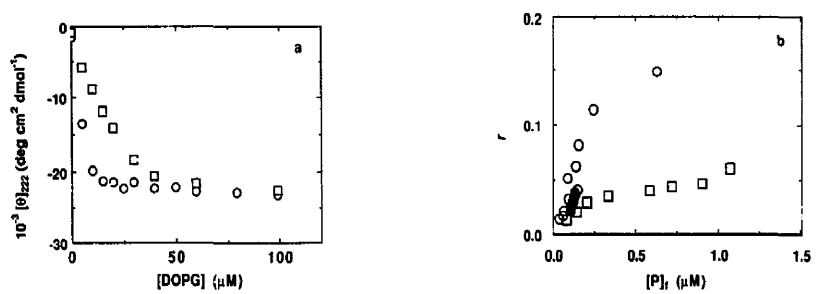

Fig. 5. Estimation of binding isotherm by titration method. (a) A magainin 1/buffer solution (1.4 μM) was titrated with a 4 mM DOPG SUV suspension. The ellipticity at 222 nm, $[\theta]_{222}$, was measured at 30°C as a function of the DOPG concentration. The buffer composition: 10 mM Tris-HCl/1 mM EDTA/150 mM (circles) or 500 mM (squares) NaCl (pH 7.0). (b) Binding isotherms at 30°C estimated from the data in (a) with the method of Beschiaschvili and Seeling [23] were shown (Symbols are the same as those in (a)) with the isotherm on the basis of the calcein leakage (closed circles, replotted from Fig. 4a).

First, we will consider the binding isotherms (Fig. 4a). The isotherms were either linear or bent downward except for the magainin 2-PS system where r was a higher order function of $[P]_f$. The latter result indicates an intramembrane peptide aggregation. For the other five isotherms, the binding affinity was evaluated by linear extrapolation of the inverse of an apparent partition coefficient, $K_{app} = r/[P]_f$, to the zero free peptide concentration (K^0_{app} values in Table I). The affinities of magainin 2 were greater than those of magainin 1 for all lipids. In each class of peptide, the K^0_{app} values were in the order DOPG > DPPG > PS.

Second, we will compare the membrane-perturbing activities (Fig. 4b). A higher activity means that the leakage occurs at a smaller r value. The activities lay in the order DOPG ≥ PS > DPPG: The fluid membranes (DOPG and PS) were leakier. The perturbing activities of magainins 1 and 2 were similar, although, for PS and DPPG, magainin 1 was slightly more active.

Effect of salt concentration

Electrostatic interactions seem to be important in the binding of magainin 1 to membranes [12]. Thus, we examined the effects of the medium's salt concentration on leakage. Fig. 6 shows that a rise in NaCl concentration inhibited leakage. This is, at least partly, ascribable to reduced binding (Fig. 5b). The $[\theta]_{222}$ values, and therefore the conformations, in the two buffers were identical for both the free and the membrane-bound states (Fig. 5a). These findings support the significant role of electrostatic interactions in the binding process.

Zeta potential

Furthermore, we determined the zeta potentials, a measure of the surface potentials, of the acidic lipid SUVs by a laser-Doppler method [18]. Table I includes potentials calculated from electrophoretic mobilities on the basis of the Smoluchowski equation [17]. Strictly, for particles of approx. 30 nm in diameter suspended in 0.15 M NaCl, the equation needs some correction [24]

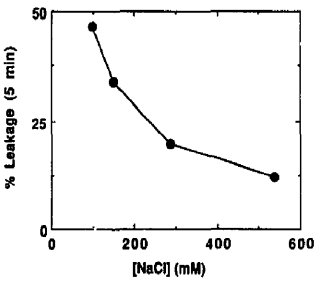

Fig. 6. Effect of salt concentration on the leakage of entrapped calcein from DOPG SUVs at 30°C. Calcein trapped DOPG SUVs were mixed with magainin 1/buffer solutions containing different concentrations of NaCl. The percent leakage values after 5 min were plotted as a function of salt concentration. The final peptide and lipid concentrations were 2.7 and 89 μM, respectively.

resulting in slightly more negative values (−10 mV for PS, −41 mM for DPPG, and −62 mV for DOPG). The order of the absolute potential values was DOPG > DPPG > PS, which coincided with the peptide-membrane affinity order (the K^0_{app} values in Table I). This observation further stresses the importance of Coulombic attractions in magainin-lipid interactions.

CD

The secondary structures of magainins 1 and 2 in their membrane-bound states will be one of the determinants for the peptide induced leakage. We studied the peptide conformations based on CD spectra. A CD spectrum measured in the presence of vesicles is a superposition of two spectra, i.e., that of the membrane-bound peptide and that of the free peptide. Thus, we extracted only the former spectrum by knowing the bound fractions of the peptides, f, from the binding isotherms (Fig. 4a): First, we measured CD spectra in the presence of the SUVs, $[\theta]_{obsd}$, then, the

TABLE I

Various parameters characterizing magainin lipid interactions

Lipid	Zeta potential [a] (mV)	Magainin	Binding [b]: $10^{-6} K^0_{app}$ (M^{-1})	Conformation [c]					
				n	% content				NRMSD
					helix	beta	turn	unordered	
DPPG	−38	1	0.093	19	83	0	9	8	0.050
	$(-2.7 \cdot 10^{-4})$	2	1.4	18	80	0	5	15	0.055
DOPG	−54	1	0.26	16	71	0	2	27	0.072
	$(-3.9 \cdot 10^{-4})$	2	3.0	16	68	0	1	31	0.090
PS	−9	1	0.040	19	85	0	1	14	0.057
	$(-0.69 \cdot 10^{-4})$	2	–	18	81	0	0	19	0.071

[a] Calculated from the observed electrophoretic mobilities (the values in parenthesis, in $cm^2\ V^{-1}\ s^{-1}$) by using the Smoluchowski equation [17].

[b] The inverse of an apparent partition coefficient, $K_{app} = r/[P]_f$, was linearly extrapolated to a zero free peptide concentration.

[c] The CD spectra of the membrane bound peptides (200–240 nm region in Figs. 7a,b) were analyzed by using a least-squares algorithm [20] with the reference spectra by Chang et al. [21]. n: helical length used in the computation. NRMSD: normalized root mean standard deviation [25].

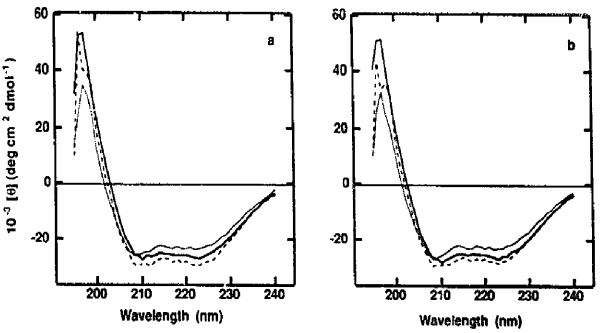

Fig. 7. CD spectra of magainins (a) 1 and (b) 2 in membrane-bound state at 30°C. The spectra were reconstructed from spectra measured in the presence and absence of SUVs by using Eqn. 2 and the binding isotherms (Fig. 4a). Each spectrum was the average for three independent preparations. Lipids: dotted lines, DOPG;solid lines, DPPG; broken lines, PS.

membrane-bound spectra, $[\theta]_{bound}$, were reconstructed according to Eqn. 2.

$$[\theta]_{bound} = \frac{[\theta]_{obsd} - (1-f)[\theta]_{free}}{f} \quad (2)$$

Here, $[\theta]_{free}$ represents the spectra measured in the buffer. The CD spectra of magainins 1 and 2 in the bound form thus obtained are shown in Figs. 7a and 7b, respectively. The measured spectra, $[\theta]_{obsd}$, were very similar to the membrane-bound spectra in Figs. 7a and 7b because the experiments were carried out under conditions where the f values exceeded 0.85.

Before interpreting the spectra, the contribution of two optical artifacts, often arising in vesicular systems, should be clarified. The first artifact, differential light scattering, can be minimized by using SUVs [25]. Under our experimental conditions, the diameters of the SUVs did not change (approx. 25 nm) upon addition of magainins as revealed by a dynamic light scattering method (a Photal laser particle analyzer LPA-3100 connected to a photon correlater LPA-3000). The presence of small vesicles does not distort CD spectra as confirmed previously [13]. The other artifact, absorption flattening, is negligible under these conditions [13]. Thus, the obtained bound form spectra (Figs. 7a and 7b), affected little by the optical artifacts, can be compared.

The CD spectra of the bound peptides were characteristic of helical conformations. The helical contents seem to be in the order (beyond reproducibility) PS ≥ DPPG ≥ DOPG, but the differences were rather small. The spectra of both peptides were very similar. This observation is compatible with the similar membrane-perturbing activities of magainins 1 and 2. The helix contents estimated by the least-squares curve fitting procedure [20] were summarized in Table I. The fitting, evaluated by the normalized root mean standard deviation (NRMSD) [25], was satisfactory (less than 0.1). As a rough estimation, 16–19 residues were involved in helix formation. (A lower helical content (58%) of the magainin 1-PS system in our previous paper [12] arises from the overestimation of the peptide concentration.) Such a curve fitting procedure gives a reasonable estimate of helicity [20], although it is problematic for exact estimation of protein secondary structures [20], especially for small peptides [22].

DSC

The effects of magainins on the gel to liquid-crystalline phase transition of DPPG multilamellar vesicles were examined by using the DSC technique (Fig. 8). In the absence of the peptides (curve 1), a sharp onset of the main transition appeared at 39.8°C with a pretransition (onset temperature 31.3°C), typical of DPPG membranes [26]. Addition of 3.5 mol% of magainin 2 abolished the pretransition and somewhat broadened the main transition while leaving the transition enthalpy (peak area) unchanged (−34.9 kJ/mol). The effect of magainin 1 was similar (data not shown). Peptides or proteins interacting with the hydrophobic regions of

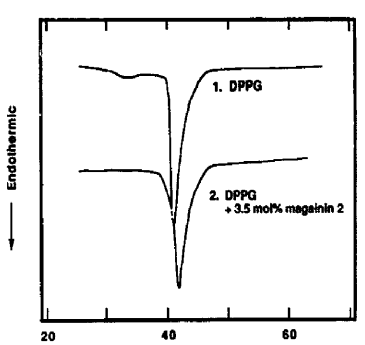

Fig. 8. DSC heating curves of DPPG multilamellar vesicles in the absence (curve 1) and presence (curve 2) of 3.5 mol% magainin 2. The heating rate was 2 C°/min.

membranes often exhibit a significant broadening of the transition with a large reduction in the transition enthalpy [13,27,28]. Thus, magainins appear to not penetrate deeply into the hydrophobic region of the DPPG bilayer.

Discussion

The action mechanism of magainins seems to be the enhancement of permeability in bacterial membranes [1–6]. Thus, an investigation of the interactions of these peptides with lipid vesicles will give us basic information on the molecular machinery of antibiotic activities. We have shown [12] that magainin 1 interacts specifically with acidic lipids to form an amphiphilic helix, inducing a change in permeability of the lipid bilayers. In this report we have systematically studied the magainin-acidic lipid interactions to elucidate what physicochemical properties in both the peptides and lipids influence the interactions.

We have examined the peptide induced enhancement of the permeability in the lipid bilayer by using leakage of a fluorescent dye, calcein, from SUVs [12,13,16]. A quantitative analysis of the leakage phenomenon provides two factors characterizing the leakage, i.e., the binding isotherm of the peptide to the membrane and the membrane-perturbing activity of the peptide [12,13]. This analysis based on Eqn. 1 assumes a fast binding equilibrium. The linearity of the $[P]_0$ vs. [L] plots (Fig. 3) guarantees validity of the assumption, as discussed previously [13]. Furthermore, we experimentally confirmed the rapid binding: We employed a leakage rate expressed as the percent leakage for the initial 1 min in the case of the fluid membranes (DOPG and PS). For these bilayers, binding isotherms obtained from the leakage rate represented as the percent leakage for the initial 5 min were superimposable onto those in Fig. 4a (data not shown). Thus, the leakage kinetics in Fig. 1 represents that of a post binding process.

The quantitative analysis (Figs. 4a and 4b) reveals a difference in susceptibility of the three acidic lipid SUVs to the peptides. First, we will consider the binding isotherms (Fig. 4a). Recent studies on peptide binding to lipid membranes introduce a model involving a partition equilibrium between free and membrane-bound peptides [23,29–32]. In the case of charged peptides, an increase in the r value reduces the binding affinity because the bound peptide charges the membranes [23,30–32], as observed in the magainin-acidic lipid systems except for the magainin 2-PS system. The affinity reducing effect has been described based on the Gouy-Chapman theory. We did not employ this type of analysis because an estimation of the surface charge densities of acidic lipid membranes is difficult because of a significant Na^+ ion binding [33]. Instead, to eliminate the negative cooperativity effect, the apparent partition coefficient, K_{app}, was extrapolated to a zero free peptide concentration (the K^0_{app} values in Table I). These values are considered to represent the binding affinities of the peptides to the membranes. The binding affinity (K^0_{app}) is mainly determined by the zeta potential of the vesicle. That is, electrostatic interactions play a crucial role in the binding. The observed difference in zeta potential may arise from the different spatial charge distributions and lipid physical states in addition to the counter ion binding: PS possesses two negative and one positive charges whereas phosphatidylglycerols possesse only one negative charge at neutral pH. The DOPG and the DPPG vesicles are in the liquid-crystalline state and in the gel state, respectively at 30°C. A more negative potential in the fluid state has been reported for dipalmitoylphosphatidylserine liposomes [34].

Furthermore, a rise in NaCl concentration reduced the binding (Fig. 5b) and the calcein leakage (Fig. 6) without affecting the peptide conformations in either the free or the bound states. These observations further stress the importance of electrostatic interactions between the peptides and the membranes. However, addition of salt appears to decrease the membrane-perturbing activity: Fig. 5b indicates that under the experimental condition in Fig. 6 ($[P]_0 = 2.7\,\mu M$, $[L] = 89\,\mu M$), the r values were reduced only slightly (from 0.029 to 0.028) upon a change in salt concentration of 150 to 500 mM. The high concentration of salt may reduce electrostatic repulsions between the lipid head groups, tightening the membrane surface region. Moreover, osmotic effect may contribute to the decreased leakage. In fact, addition of sorbitol to the extravesicular medium somewhat diminished the leakage (data not shown).

Next, the membrane-perturbing activity appears to be regulated by membrane fluidity: The fluid membranes (DOPG and PS) are leakier. The secondary structures of the bound peptides are similar, containing approx. 16–19 residues helices, although the helical lengths are somewhat longer in membranes with lower surface charge densities. In the fluid membranes, magainins 1 and 2 may be inserted deeper into the hydrophobic region, further disrupting the lipid organization. Interestingly, these findings form a striking contrast to the observations of a hydrophobic peptide, hypelcin A [13]: The leakage-occurring r values for hypelcin A (10^{-3}–10^{-2}) are much smaller than those for magainins (10^{-2}–10^{-1}, Fig. 4b). Furthermore, hypelcin A more effectively disrupts the lipid bilayer organization in the gel state. A possible explanation is as follows: the hydrophobic peptide penetrates deeply into the hydrophobic region, causing lipid packing defects which cannot be repaired effectively by the surrounding solid lipids. On the other hand, charged amphiphilic magainins interact with the acidic bilayers in their surface region: The amphiphilic helix, with its axis parallel to

the membrane surface, penetrates relatively shallowly into the hydrophobic region, weakly disrupting the lipid organization. The DSC data (Fig. 8) indicate that a modification of the membrane phase transition is rather small compared with the hypelcin A- dipalmitoylphosphatidylcholine system [13]. A recent Raman study [35] reported that magainin 2 amide appears to bind to the surface of liposomes without spontaneously penetrating the bilayers. Gel state membranes (DPPG) with strong interlipid interactions inhibit deep insertion of magainins, thus are more resistant to magainins. Bee venom melittin, an amphiphilic membrane-lytic peptide, preferentially associates with fluid state lipids [36]. Salmon calcitonin, which shows specific interactions with acidic lipids, can react with phosphatidylglycerol membranes at or above their gel to liquid-crystalline phase transition temperatures [26].

The apparent differences in membrane-lytic potency between magainins 1 and 2 can be understood clearly on the basis of our quantitative analysis. The affinities (K^0_{app}) of magainin 2 to the membranes are an order of magnitude larger than those of magainin 1 in spite of the same net charge. Molecular level consideration of the peptide-membrane interaction mode can explain this difference. The amino acid sequences show that magainins contain two regions, i.e., 14 positively charged residues from the N-terminal and five negative charge-bearing C-terminal residues. The latter domains should be expelled from the membrane surfaces by electrostatic repulsions. The former regions can form amphiphilic helices, interacting with negatively charged membranes. Indeed, the CD data (Table I) suggest that the helical lengths are at least 14 but not exceeding 19 residues irrespective of the systems studied. Williams et al. estimated an upper limit of helical length for membrane-bound magainin 2 amide to be 16 residues [35]. The helical contents are somewhat larger in membranes with smaller absolute zeta potential values (Table I). This finding further supports the above picture of the reduced repulsions between the C-terminal regions and the membranes enhancing the helical folding of intermediate regions between the positively charged and the negatively charged portions. Magainin 2, binding more strongly to acidic lipids, possesses six positive charges in the N-terminal region whereas magainin 1 bears five. If the C-terminal charges are repulsed from the membrane surfaces, they do not contribute significantly to the binding energies because the presence of salt (0.15 M) effectively shields the electrostatic interactions (the Debye length is 0.8 nm). The above picture can explain several observations: Magainin 2 is more active than magainin 1 [2]; A free α-amino terminus is required for maximal activity [8]; And furthermore, a truncated magainin 2 (residues 5–23) shows only a weak antimicrobial activity compared with longer peptides as reported by Zasloff et al. [2]. They concluded that at least 20 residues are required for activity, but the loss of Lys^4, a positively charged residue, may be in part ascribed to the reduced potency.

Finally, the leakage mechanism will be considered. Peptide-induced change in permeability sometimes accompanies fusion of vesicles [10,37,38]. In the case of the PS SUVs, the 90° light scattering intensities were unchanged under conditions where the percent leakage values for the initial 1 min were less than 40%. This finding strongly demonstrates that neither fusion nor solubilization is the leakage mechanism. However, when the percent leakage values exceeded 40%, slight increases in light scattering were observed, suggesting the occurrence of aggregation or fusion of the SUVs, which is probably responsible for the inflections in the percent leakage-r curves (Fig. 4b).

Our quantitative study shows that several hundred peptide molecules must accumulate for leakage (Fig. 4b). This implies two possibilities. The first is a monomer-aggregated channel mechanism [6,7]. For charged peptides, even a significant extent of aggregation can give a downward-bent binding isotherm because of the negative cooperative effect [32]. The other plausible mechanism is a monomer induced disruption of the lipid organization. Binding of a single monomeric peptide causes a small local perturbation of lipid packing in close vicinity of the peptide. The individual disrupted site cannot significantly enhance membrane permeability. Accumulation of the monomers leads to site-site interactions which create much leakier patches, not channel pores, in the bilayers. The latter mechanism may be favored because of the finding that the membrane-perturbing activity of the magainin 2-PS system, where the binding isotherm is indicative of an intramembrane peptide aggregation (Fig. 4a), is somewhat smaller than that of the magainin 1-PS system. Williams et al. [35] reached a similar conclusion. However, elucidation of the leakage mechanism, by another experimental approach, is a subject of continuing study. Furthermore, the presence of a transmembrane potential might alter aggregational states, orientations, and conformations of the peptides in membranes [29,39].

In conclusion, we hypothesize a tentative model for the interactions of magainins 1 and 2 with membranes. First, the positively charged N-terminal regions (at least 14 residues) interact with the negatively charged surfaces of acidic lipid membranes to form amphiphilic helices. Electrostatic interactions play a crucial role in this binding process: The positive charges in the N-terminal regions and the membrane surface potentials as well as a medium salt concentration affect the binding affinities. Then, the formed hydrophobic surfaces in the helical rods are incorporated shallowly into the hydrophobic regions of the membranes with the helical axes parallel to the membrane surfaces. The incorporated peptides induce an enhancement in permeability. We

are now testing the above model by using several magainin analogues.

Acknowledgements

This work was supported in part by a Grant-in Aid (No. 02453144) for Scientific Research from the Ministry of Education, Science and Culture of Japan. We thank Dr. T. Handa for his helpful discussion and Mr. H. Tokuda for his experimental assistance.

References

1 Zasloff, M. (1987) Proc. Natl. Acad. Sci. USA 84, 5449–5453.
2 Zasloff, M., Martin, B. and Chen, H.-C. (1988) Proc. Natl. Acad. Sci. USA 85, 910–913.
3 Juretić, D.J., Chen, H.-C., Brown, J.H., Morell, J.L., Hendler, R.W. and Westerhoff, H.V. (1989) FEBS Lett. 249, 219–223.
4 Westerhoff, H.V., Juretić, D., Hendler, R.W. and Zasloff, M. (1989) Proc. Natl. Acad. Sci. USA 86, 6597–6601.
5 Westerhoff, H.V., Hendler, R.W., Zasloff, M. and Juretić, D. (1989) Biochim. Biophys. Acta 975, 361–369.
6 Cruciani, R.A., Stanley, E.F., Zasloff, M., Lewis, D.L. and Baker, J.L. (1988) Biophys. J. 53, 9a.
7 Duclohier, H., Molle, G. and Spach, G. (1989) Biophys. J. 56, 1017–1021.
8 Chen, H.-C., Brown, J.H., Morell, J.L. and Huang, C.M. (1988) FEBS Lett. 236, 462–466.
9 Kanellis, P., Romans, A.Y., Johnson, B.J., Kercret, H. and Chiovetti, R., Jr. (1980) J. Biol. Chem. 255, 11464–11472.
10 Kubesch, P., Boggs, J., Luciano, L., Maass, G. and Tümmler, B. (1987) Biochemistry 26, 2139–2149.
11 Subbarao, N.K., Parente, R.A., Szoka, F.C., Jr., Nadasdi, L. and Pongracz, K. (1987) Biochemistry 26, 2964–2972.
12 Matsuzaki, K., Harada, M., Handa, T., Funakoshi, S., Fujii, N., Yajima, H. and Miyajima, K. (1989) Biochim. Biophys. Acta 981, 130–134.
13 Matsuzaki, K., Nakai, S., Handa, T., Takaishi, Y., Fujita, T. and Miyajima, K. (1989) Biochemistry 28, 9392–9398.
14 Ratledge, C. and Wilkinson, S.G. (eds.) (1988) Microbial Lipids, Vol. 1, Academic Press, London.
15 Bartlett, G.R. (1959) J. Biol. Chem. 234, 466–468.
16 Allen, T.M. and Cleland, L.G. (1980) Biochim. Biophys. Acta 597, 418–426.
17 Adamson, A.W. (1967) Physical Chemistry of Surfaces, 2nd Edn., Ch. 8, Interscience Publishers, New York.
18 Imae, T., Otani, W. and Oka, K. (1990) J. Phys. Chem. 94, 853–855.
19 Takakuwa, T., Konno, T. and Meguro, H. (1985) Anal. Sci. 1, 215–218.
20 Yang, J.T., Wu, C.-S.C. and Martinez, H.M. (1986) Methods Enzymol. 130, 208–269.
21 Chang, C.T., Wu, C. and Yang, J.T. (1978) Anal. Biochem. 91, 13–31
22 Cascio, M. and Wallace, B.A. (1988) Proteins: Struct., Funct., Genet. 4, 89–98.
23 Beschiaschvili, G. and Seeling, J. (1990) Biochemistry 29, 52–58.
24 Wiersema, P.H., Loeb, A.L. and Overbeek, J.T.G. (1966) J. Colloid Interface Sci. 22, 78–99.
25 Mao, D. and Wallace, B.A. (1984) Biochemistry 23, 2667–2673.
26 Epand, R.M., Epand, R.F., Orlowski, R.C., Schlueter, R.J., Boni, L.T. and Hui, S.W. (1983) Biochemistry 22, 5074–5084.
27 Alonso, A., Restall, C.J., Turner, M., Gomez-Fernandez, J.C., Goñi, F.M. and Chapman, D. (1982) Biochim. Biophys. Acta 689, 283–289.
28 Chapman, D., Cornell, B.A., Eliasz, A.W. and Perry, A. (1977) J. Mol. Biol. 113, 517–538.
29 Rizzo, V., Stankowski, S. and Schwartz, G. (1987) Biochemistry 26, 2751–2759.
30 Kuchinka, E. and Seeling, J. (1989) Biochemistry 28, 4216–4221.
31 Stankowski, S. and Schwarz, G. (1990) Biochim. Biophys. Acta 1025, 164–172.
32 Schwarz, G. and Beschiaschvili, G. (1989) Biochim. Biophys. Acta 979, 82–90.
33 Kurland, R., Newton, C., Nir, S. and Papahadjopoulos, D. (1979) Biochim. Biophys. Acta 551, 137–147.
34 MacDonald, R.C., Simon, S.A. and Baer, E. (1976) Biochemistry 15, 885–891.
35 Williams, R.W., Starman, R., Taylor, K.M.P., Gable, K., Beeler, T. and Zasloff, M. (1990) Biochemistry 29, 4490–4496.
36 Schulze, J., Mischeck, U., Wigand, S. and Galla, H.-J. (1987) Biochim. Biophys. Acta 901, 101–111.
37 Parente, R.A., Nir, S. and Szoka, F.C., Jr. (1988) J. Biol. Chem. 263, 4724–4730.
38 Eytan, G.D., Broza, R. and Shalitin, Y. (1988) Biochim. Biophys. Acta 937, 387–397.
39 Kempf, C., Klausner, R.D., Weinstein, J.N., Renswoude, J.V., Pincus, M. and Blumenthal, R. (1982) J. Biol. Chem. 257, 2469–2476.